Morphology–Property Relationship in Oriented PET Films: Microstructural Reorganization during Heat Treatment

RAMESH M. GOHIL

DuPont Co., Circleville Research Laboratory, Circleville, Ohio 43113

SYNOPSIS

Morphology–property relationships for simultaneously biaxially stretched films and heat-set with fixed dimensions in the temperature range of 100–240°C have been studied. The observed transition in various properties at 180°C can be explained on the basis of microstructural changes caused by competition among several processes, such as crystallization, solid-state thickening, melting, and molecular relaxation as well as by melting and recrystallization. The resulting structures and, thereby, the properties are different in temperature Regime-II (T_g to T_{max}) and Regime-III (T_{max} to T_m). In Regime-II, the high rate of crystallization compared to the rate of molecular relaxation develops a constrained amorphous phase, whereas the predominant melting and recrystallization process in Regime-III generates the relaxed amorphous phase. The structural reorganization during heat treatment is almost the same for uniaxially oriented film, fibers, and biaxially oriented films prepared under similar processing conditions. © 1994 John Wiley & Sons, Inc.

INTRODUCTION

The present article forms a part of our series of papers on oriented poly(ethylene terephthalate) (PET) films.[1-4]

There is extensive interest in understanding the structures and their reorganization during heat treatment of uniaxially oriented PET fibers and films[5-20] as well as biaxially oriented PET films.[21-29] The structures of films obtained immediately after the stretching process, either uniaxially or biaxially, are metastable, i.e., far from thermodynamic equilibrium. These structures are converted to the thermodynamically more stable structures via heat-setting or annealing. Final dimensional stability and other properties of the films and fibers are set at this stage. The extent of the reorganization is determined by the details of the heat-setting process, e.g., heat-setting with fixed dimension, under tension, in a relaxed state, and in different atmospheres. The major structural variables controlling the properties of the film are the initial molecular orientation; the percent crystallinity; the crystal size, shape, and perfection; the length of the amorphous region; and the state of the amorphous phase and its distribution in the film plane. Besides the stretching and heat treatments, the polymeric formulation also plays an important role in achieving the final film properties. The polymer formulation includes the concentrations of carboxylic acid, catalyst deactivant, unreacted catalyst, and slip additives, as well as the diethylene glycol (DEG) copolymer content in PET and the molecular weight of the polymer.

In uniaxially oriented PET films, one observes micellar- or fibrillar-type crystals.[5] On heat treatment, these crystals have a tendency to fuse, and at a higher annealing temperature, fibrillar crystals transform into lamellar crystals. The lamellar crystals on further heat treatment reorganize via melting and recrystallization processes. At this stage, it is useful to describe the basic reorganization process via melting and recrystallization. Uniaxially oriented films of polyethylene-containing lamellar crystals have been investigated directly by hot-stage electron microscopy.[30] The basic reorganization process was similar to that noted in the lamellae of spherulites.[31] In this process, (a) sandwiched lamellae are eaten up by the adjacent thickening lamellae; (b) structural irregularities on the crystal surface hinder the

Journal of Applied Polymer Science, Vol. 52, 925–944 (1994)
 CCC 0021-8995/94/070925-20

solid-state crystal thickening process and those local areas melt preferentially; (c) the elastically bent part of a lamella melts preferentially; and (d) thinner areas in a lamella melt-out preferentially.

In the present study, the properties of simultaneously biaxially oriented PET films have been investigated as a function of annealing temperature or heat-set temperature (HST). The major difference between the sequential and the simultaneous stretching process is that the former involves stretching of already crystallized uniaxially stretched film.[1] Here, the isotropic in-plane orientation occurs before achieving an equal draw ratio in both orthogonal directions. In the simultaneous stretching process, the in-plane crystal and molecular orientation is equal at all equal draw ratios; thus, one achieves isotropic in-plane properties.[1]

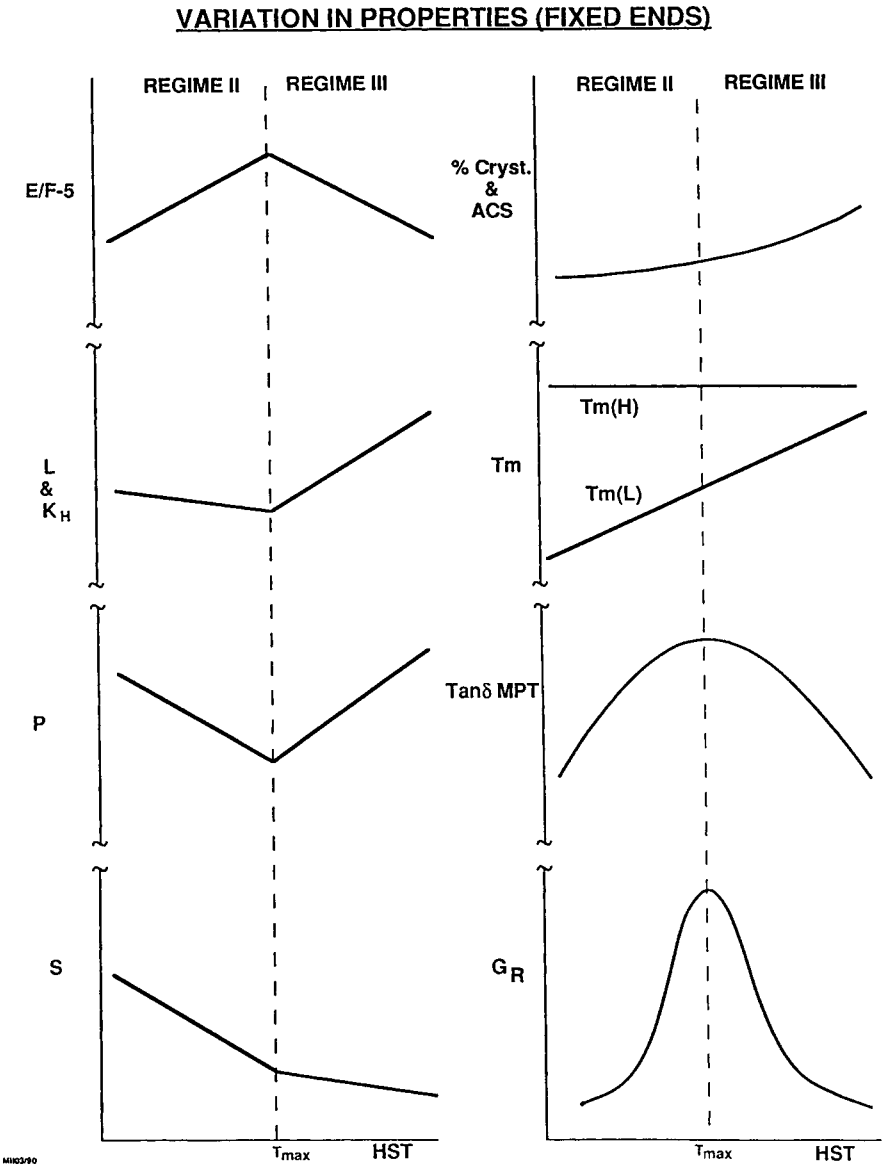

Figure 1 Schematic representation of variations in different properties with heat-set temperatures. E = tensile modulus, F-5 = stress at 5% strain, L = long spacings, P = oxygen permeability, S = shrinkage, ACS = apparent crystal size, K_h = rate of hydrolysis, T_m = melting temperature, % cryst. = percent crystallinity, tan δ max PT = tan δ maximum peak temperature measured from tan δ-temperature curves obtained from dynamic mechanical analysis, HST = heat-set temperature, GR = growth rate from relaxed state.

The general trends in the various properties are shown schematically in Figure 1. Properties attain a maximum or minimum at the temperature (T_{max}) where the rate of crystallization reaches its highest value. The tensile modulus and the stress at 5% strain (F-5) increase up to T_{max} and then decrease. A similar situation is noted in the values of the temperature at which tan δ reaches its maximum. Oxygen permeability follows the inverse trend. The rates of hydrolysis and the long spacings measured from the small-angle X-ray scattering remain almost constant up to T_{max} and then they become a strong function of annealing temperature. The shrinkage rapidly decreases up to T_{max} and then it slows down. The understanding of morphology–property relationships and the major cause of the transition in the different properties in the temperature range of 180–190°C is the major aim of this communication. This observed behavior in biaxially oriented films will be compared with the results noted in fibers and in uniaxially oriented films.

EXPERIMENTAL

Films used in the present study were stretched simultaneously in the machine direction (MD) and transverse direction (TD) at 95°C and at a rate of 9000%/min. The draw ratios along the MD and TD were kept at 3.4 and 3.5, respectively.

X-Ray

Pole figures were obtained with a Picker "single-crystal" goniometer with Eulerian geometry and three axes (phi, chi, and two-theta) automated. Ni-filtered copper radiation was used as the X-ray source. A specimen is mounted in the instrument and aligned so that the MD is coincident with the direction $\chi = 90$ (the north pole–south pole axis) and the surface normal (SN) or "thickness direction" (ThD) is directed along $\phi = 0$, $\chi = 0$; the TD is then along $\phi = 90$, $\chi = 0$. Details regarding sample preparation, definitions of various directions, and angles have been discussed previously.[1,2]

For studying crystalline reorganization, pole figure analyses of the (100), ($\bar{1}$05), and (110) planes were carried out. The ($\bar{1}$05) reflection is the most suitable for monitoring the c-axis orientation. In uniaxially oriented films, the c-axis (molecular direction) is mainly along the MD (along the north–south direction). In such a case, one observes intensity from the ($\bar{1}$05) planes in the plane of a great circle (see Fig. 2 of Ref. 2). The spread in intensity indicates a deviation of the c-axis from the plane of the film. If crystals are oriented along both directions, MD and TD, then one observes a bimodal distribution in the intensity. A film having isotropic crystal orientation in the film plane will show a continuous band of uniform intensity in the plane containing a great circle having highest radius.[1]

Wide- and small-angle X-ray scattering experiments were conducted in the transmission mode, using CuKα radiation. For small-angle X-ray scattering (SAXS) measurements, a Kratky camera was used. CuKα (45 kV, 40 mA, Ni filter) and a slit system containing a slit width of 120 μ were used. Single sheets of PET film (approximately 1 mm thick) were used for the SAXS exposures. The crystal size (width) is determined from the half-width of the WAXS (100) diffraction peak, using Scherrer's equation. Data were obtained in reflection from a single layer of film using a powder diffractometer.

Density Measurements

The densities of the PET films were obtained using a density gradient column made from toluene and carbon tetrachloride. The percentage crystallinity of the films was computed from

$$X = \frac{\rho_c(\rho - \rho_a)}{\rho\,(\rho_c - \rho_a)} \times 100$$

where ρ is the density. The subscripts "c" and "a" denote the crystalline and amorphous phases, respectively. For other details, refer to the previous article.[1]

Permeability Measurements

The apparatus used in the present work was a Mocon Ox-Tran Twin DL 200 oxygen permeability tester. Measurements were carried out at 25°C. A 4 × 4 in. film is placed between the two halves of the chamber, and the chamber and film sample are flushed with a carrier gas (nitrogen with a trace of hydrogen) to completely remove all traces of oxygen. In the cell, oxygen is introduced to one surface at a pressure of 1 atm and the oxygen emerging from the opposite surface is carried away by the carrier gas to a sensor, which gives a measurement of oxygen content.[2] All the reported permeabilities were normalized for the thickness of the individual films and expressed as cubic centimeters of gas transmitted through 100 sq in. of barrier per day at a pressure differential of one atmosphere and a thickness of 1 mil. It is denoted as cc-mil/100 sq in. 24 h-atm.

Differential Scanning Calorimeter (DSC)

A DuPont DSC 2910 instrument was used for thermal characterization of the films. All samples were scanned using a heating rate of 20°C per minute. To study the thermal behavior of PET film with fixed ends, a narrow strip of PET film is wrapped on the aluminum sheet and tightened with aluminum wire. A similar procedure was used for polybutene-1.[32]

Thermal Mechanical Analyzer

Dimensional changes in the films were measured as a function of temperature using a DuPont 2940 thermal mechanical analyzer (TMA). The heating rate during the TMA scan was 20°C/min and the force applied to the sample was 0.05 N.

Dynamic Mechanical Analysis

Dynamic mechanical analysis (DMA) was carried out using a Polymer Lab DMTA instrument in the temperature range of 0–250°C using a frequency of 1 Hz, a heating rate of 5°C/min, and sample dimensions of 5.67 × 2 mm.

Mechanical Properties

The mechanical measurements were carried out on film samples (2.5 × 5.0 cm) with a Model 1122 Instron machine at room temperature using a strain rate of 100%/min.

Rate of Hydrolysis

PET films were kept in the boiling water for different periods of time. The rate of hydrolysis was followed by measuring the change in the intrinsic viscosity.

RESULTS

In the present study, biaxially oriented PET films having in-plane isotropic properties were heat-set

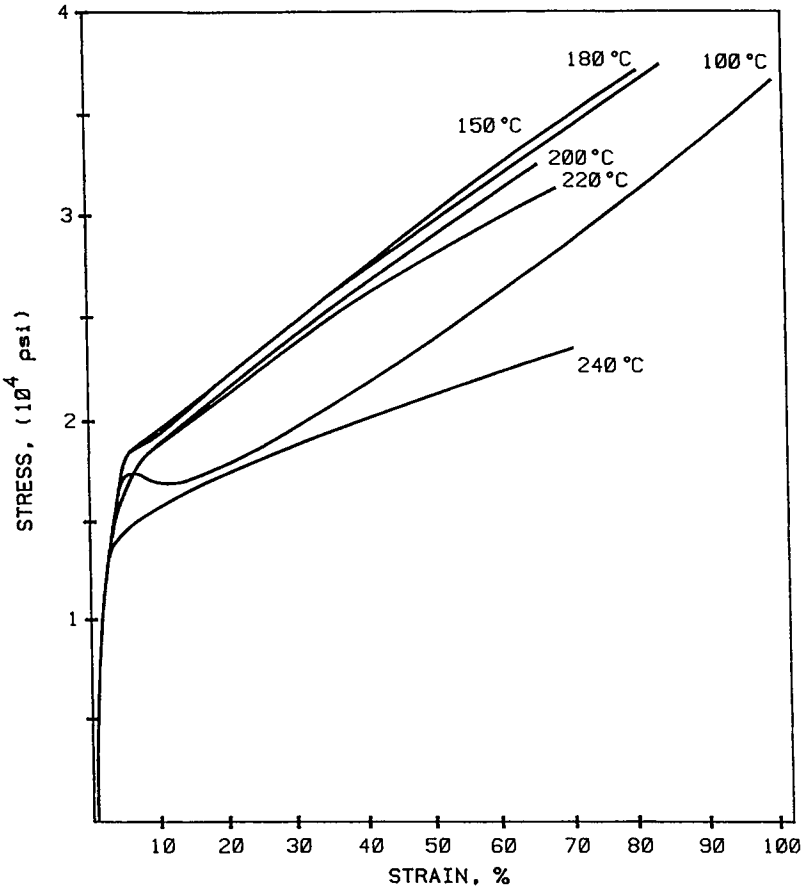

Figure 2 Stress–strain curves along the MD for the films heat-set at different temperatures.

with fixed dimensions in the temperature range of 100–240°C. The major changes in properties and structure with annealing or heat-set temperature (HST) are summarized below:

- Stress–strain curves along the MD of the films heat-set at the different temperatures are depicted in Figure 2. The tensile modulus and the values of F-5 (stress at 5% strain) are shown in Figure 3. A similar trend is noted along the TD. The tensile modulus and tensile properties slowly increase up to 180°C and then decrease. The strain hardening, which starts decreasing above 180°C, is a function of HST. The percentage elongation at break lies in the range of 60–100%.
- TMA traces showing dimensional changes along the MD with heat-set temperatures are compiled in Figure 4(a), whereas the percentage shrinkage measured at 100 and 150°C as a function of HST is plotted in Figure 4(b). There is a very rapid decrease in the shrinkage up to 180°C; then, its rate slows. The change in the slopes above and below 180°C in Figure 4(b) reflects two different mechanisms controlling the film shrinkage. A similar trend in shrinkage is noted along the TD.
- The measurements of oxygen permeability of the films heat-set at different temperatures are shown in Figure 5. The oxygen permeability attains a minimum value at about 180°C. The measurements of oxygen permeability indi-

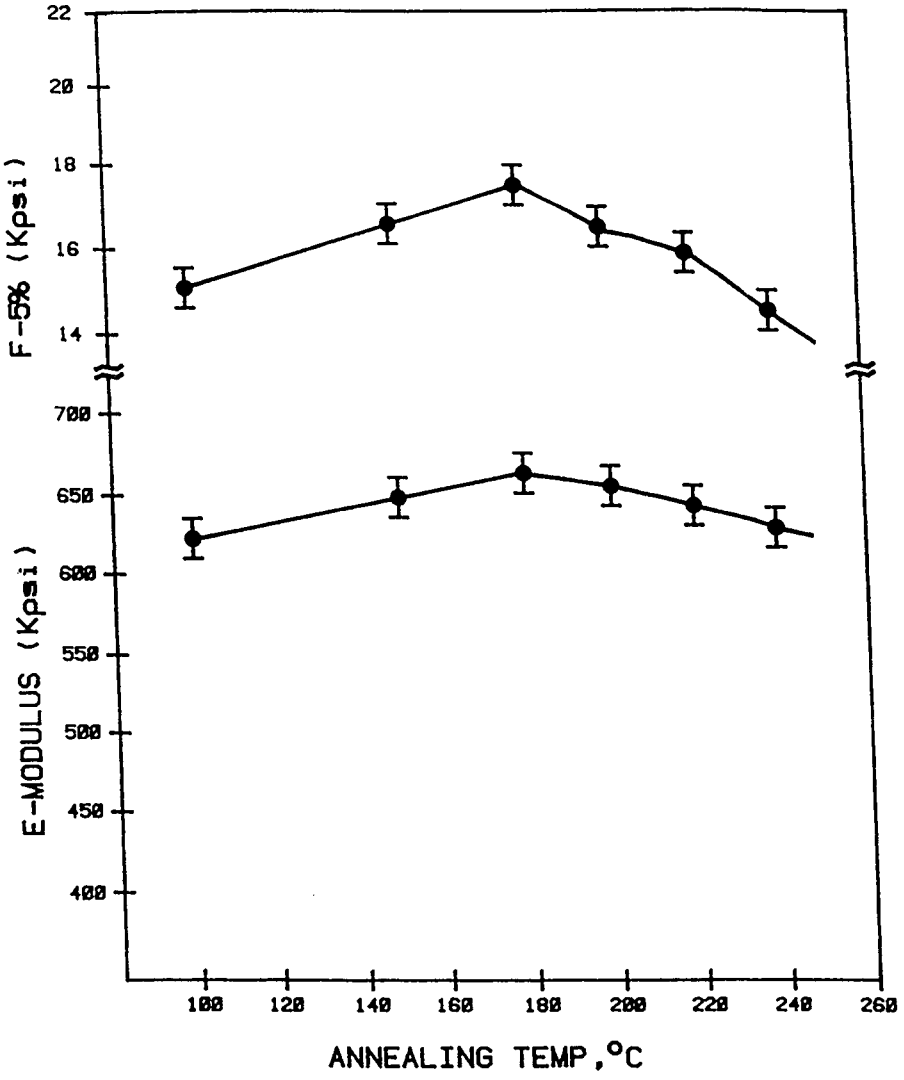

Figure 3 Variation in the tensile modulus and in the values of F-5 (stress at 5% strain) as a function of HST.

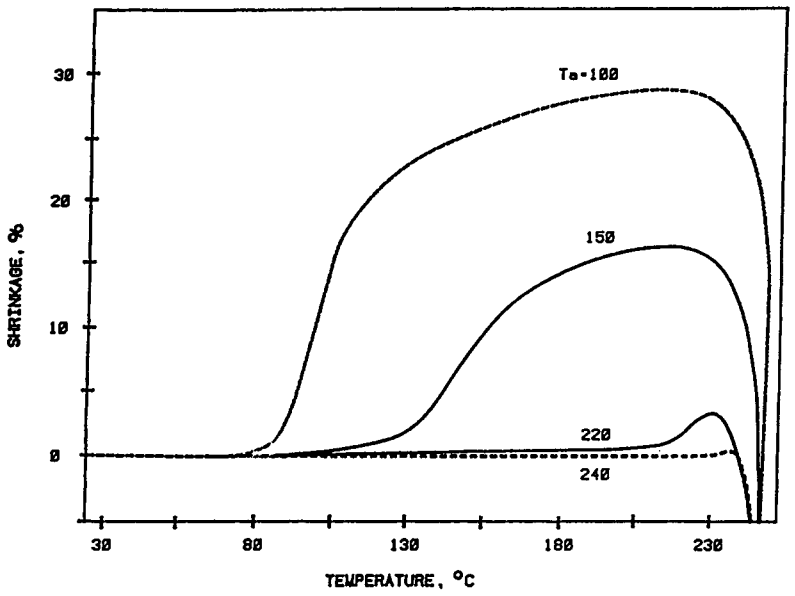

a)

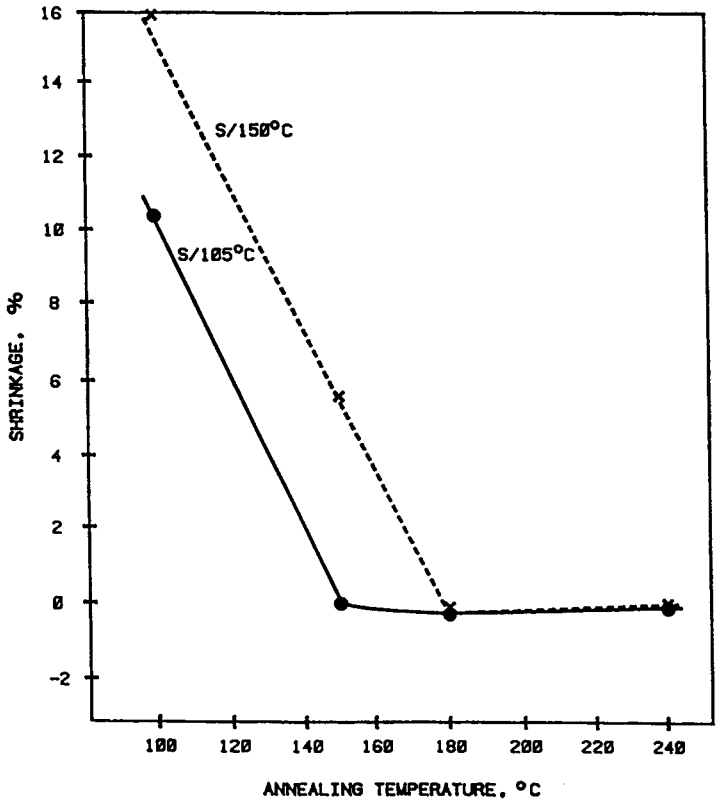

b)

Figure 4 (a) TMA traces of the film heat-set at the different temperatures. T_a = annealing temperature. (b) Variation in % shrinkage as a function of HST. Results were obtained from TMA curves for the shrinkage at 105 and 150°C. S = shrinkage.

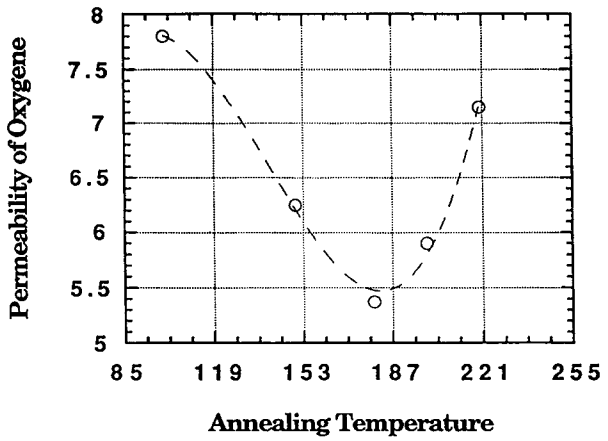

Figure 5 Variation in the oxygen permeability with HST.

rectly reflect the changes taking place in the amorphous phase.

- Long spacings, measured from the SAXS study for films heat-set at different HST are shown in Figure 6. There is a very slight change in the values of the long spacings up to 180°C and then it becomes a strong function of HST.
- The rate of hydrolysis of films heat-set at different temperatures is shown in Figure 7. The variation in the rates of hydrolysis with HST temperature is similar to that noted for the long spacings.
- DMA traces of tan δ-temperature along the TD for the films heat-set at different HST are shown in Figure 8(a), whereas the tan δ maximum peak temperatures measured from DMA traces for the films heat-set at different temperatures are shown in Figure 8(b). The measurements were carried out in three different directions in the plane of the films: They are the MD, the TD, and along the optic axis (OA), where the refractive index shows highest value in the film plane. The results give information about the degree of anisotropy in molecular orientation in the film plane. Along all the three directions, the values tan δ maximum peak temperature attain a maximum at 180°C. This high temperature denotes the development of a high degree of constraint in the amorphous phase.
- The values of percent crystallinity of the films heat-set at different temperatures are shown in Figure 9. The crystallinity increases continuously with HST.
- Lateral sizes of the crystallites measured from X-ray diffractometer scans are plotted in Figure 10. These values of apparent crystal size also continuously increase with HST.
- DSC traces of the film scanned under relaxed state, as well as under constant dimensions, are compiled in Figure 11(a). In both cases, the difference in melting points is less than 2°C. This reflects that the structure developed in the films does not induce significant superheating. The variation in the observed melting points are plotted in Figure 11(b) as a function of HST. The temperature of the endothermic peaks at the higher temperatures remains almost constant [Fig. 10(b)], whereas that observed at lower temperatures is a strong function of HST.

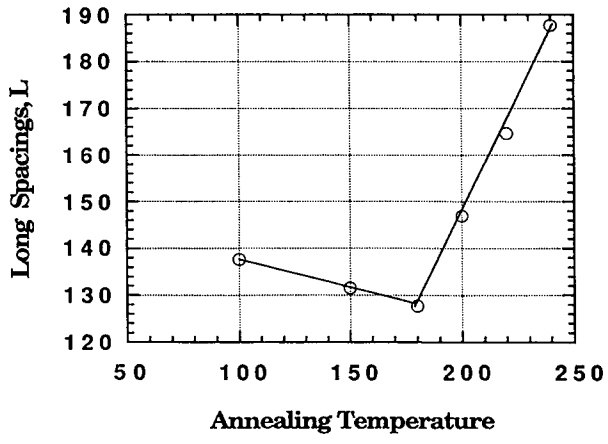

Figure 6 Variation in the long spacings (L) measured from SAXS as a function of HST.

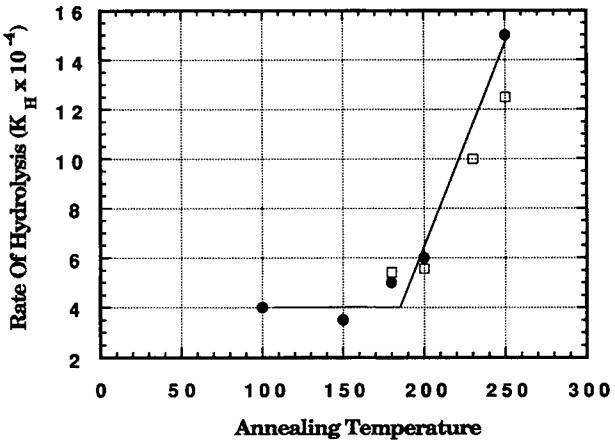

Figure 7 Variation in the rate of hydrolysis (K_h) with the annealing temperature. Open points are for sequentially stretched films.

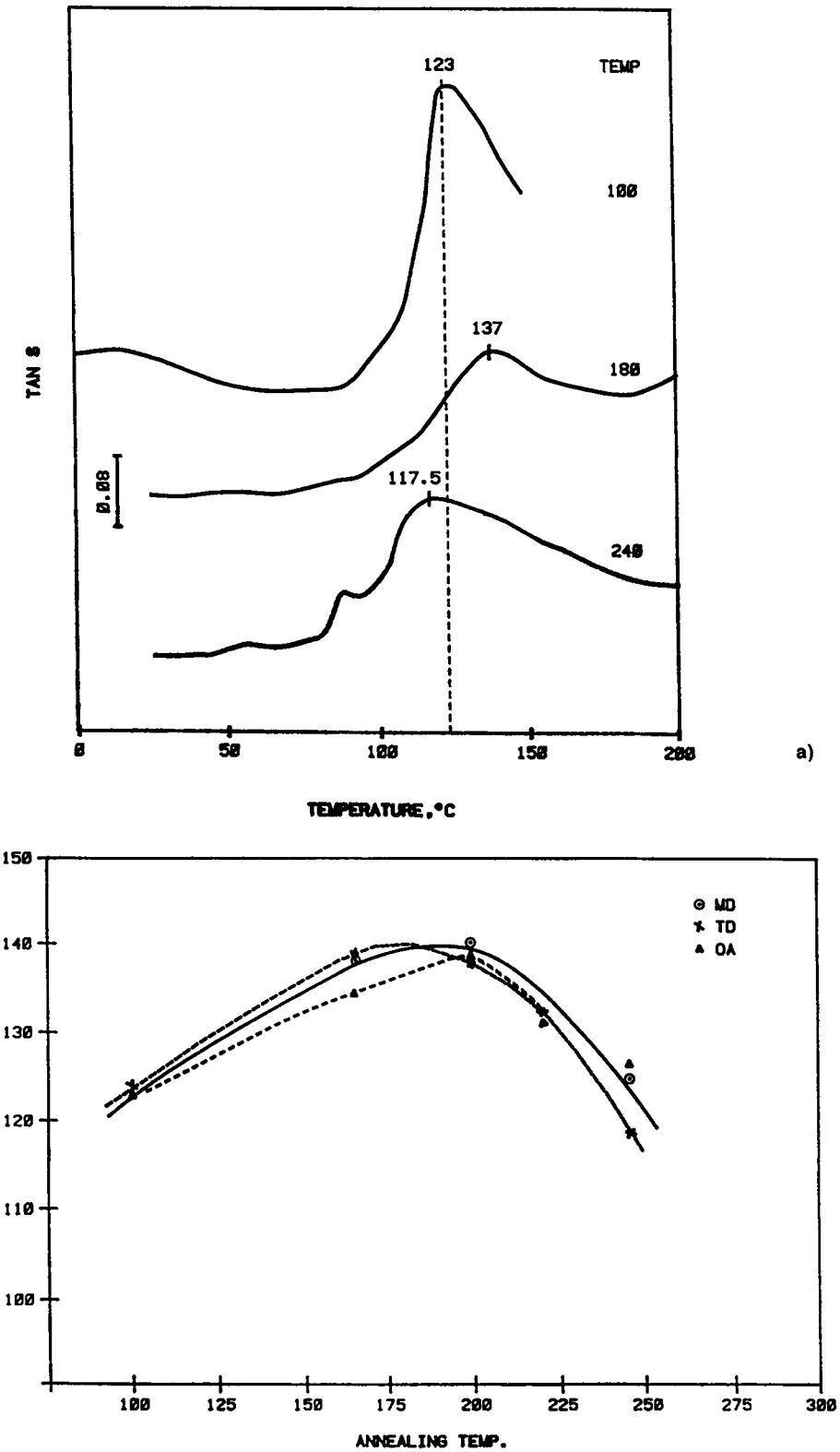

Figure 8 (a) Tan δ-temperature curves from dynamic mechanical analysis for the film heat-set at different temperatures. Heat-set temperatures are shown on the right-hand side. (b) Tan δ maximum peak temperature obtained from DMA traces as a function of HST.

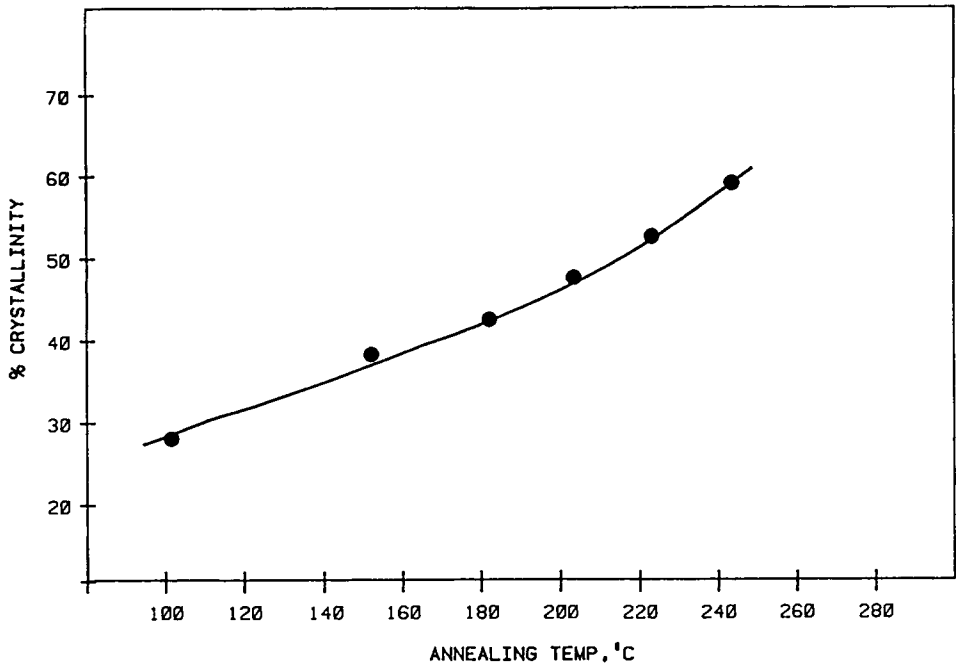

Figure 9 Variation in % crystallinity as a function of HST.

- The infrared band at 988 cm^{-1} has been shown to represent chain-folding in PET.[33] The effect of heat-set temperature on the above IR band is shown in Figure 12. With increasing HST above 180°C, the intensity of the band increases, indicating an increase in the volume fraction of crystals with chain-folded lamellar crystals.

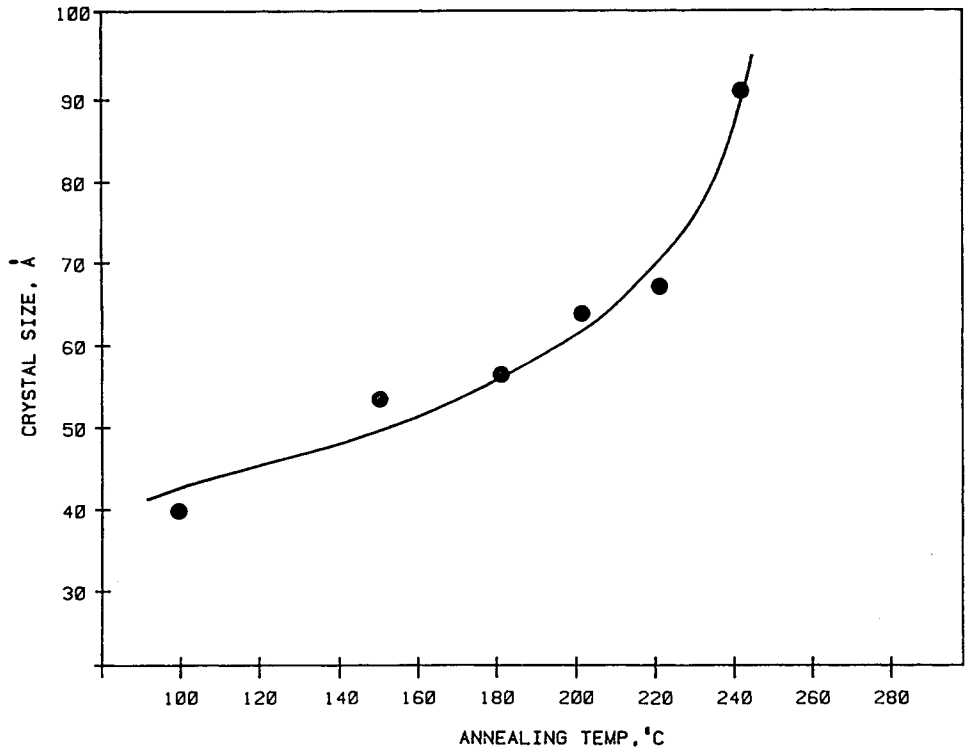

Figure 10 Variation in the apparent crystal size (ACS) as a function of HST.

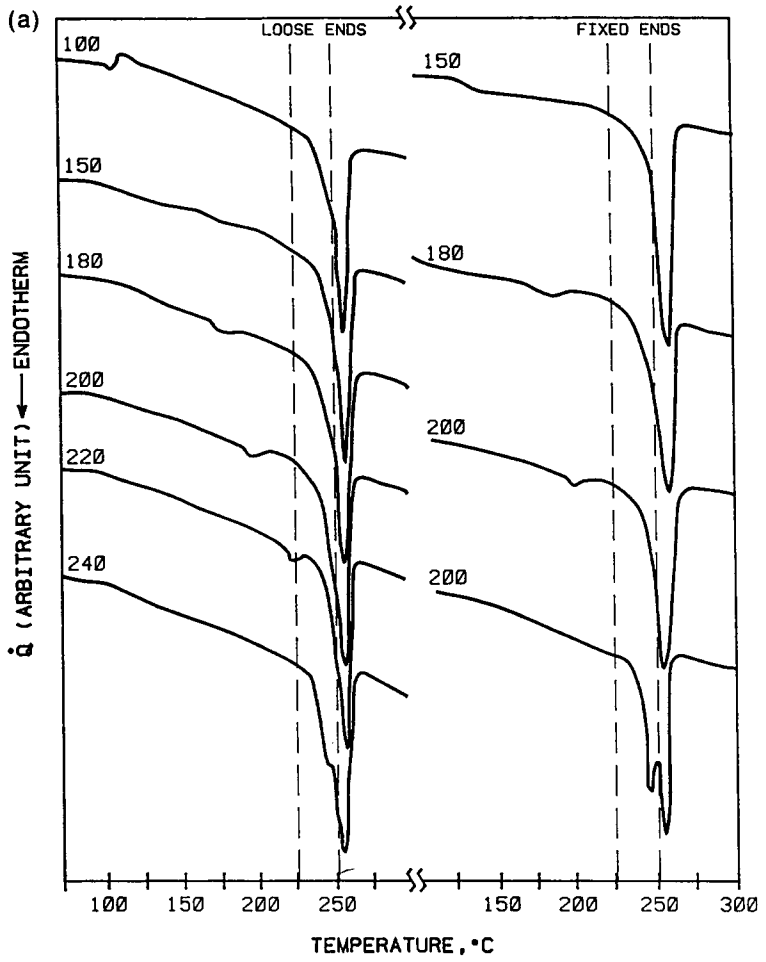

Figure 11 (a) DSC traces taken with the loose ends and the fixed ends of the films heat-set at the different temperatures. (b) Variation in the temperature of endothermic peak as a function of HST.

- The changes taking place in the crystal orientation with respect to the film plane during heat-setting can be monitored from wide-angle X-ray pole figures (WAXPF). For details, refer to previous publications.[1,2] (100), ($\bar{1}$05), and ($\bar{1}$10) pole figures of the films heat-set at different temperatures are depicted in Figure 13. (100) pole figures indicate that with increasing heat-treatment the (100) plane lies increasingly more parallel with the film plane, i.e., the planarity of the film increases with HST. ($\bar{1}$05) pole figures show the *c*-axis orientation of crystallites. There are no appreciable changes in the *c*-axis orientation in the film plane, i.e., the original *c*-axis orientation of crystallites is maintained during heat treatment. ($\bar{1}$10) pole figures also support the suggestion that on heat treatment the original orientation of crystallites is not greatly modified.
- Wide-angle X-ray scattering patterns of films heat-set at different temperatures are shown in Figure 14(a), whereas diffractometer scans along the MD are shown in Figure 14(b). Arrows in the figure indicate the MD. With increasing HST, X-ray reflections become sharper. The apparent crystallite size varies from 50 to 90 Å.
- Intrinsic fluorescence study shows a decrease in the orientation of the amorphous phase when heated above 180°C.[3]
- Optical microscopy and small-angle light-scattering study do not show the presence of spherulitic structure in the films.

So far, we have presented our results on simultaneous biaxially stretched films. In order to generalize the reorganization process, it may be useful

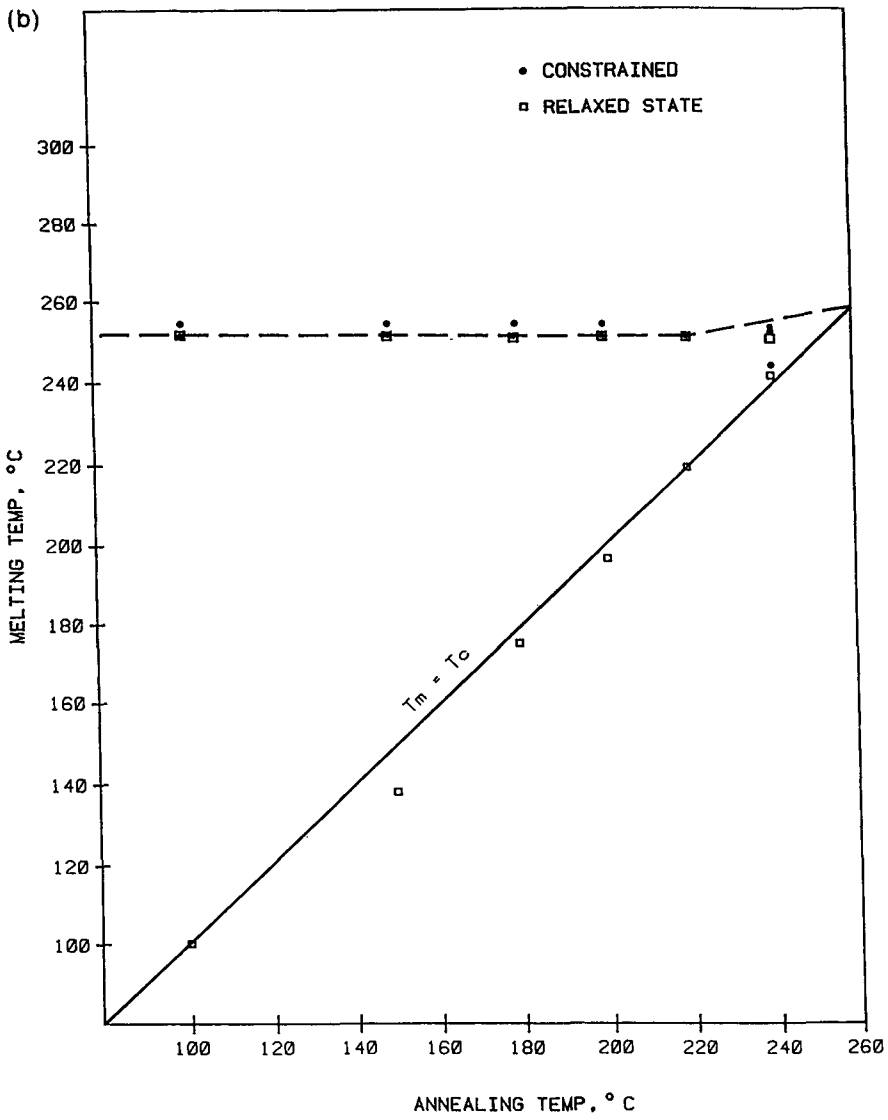

Figure 11 *(Continued from the previous page)*

to highlight some of the previously reported important results on uniaxially oriented films and fibers:

- Electron microscopic and X-ray studies on the uniaxially oriented fibers and films[4,5,19] reveal the presence of micellar or needlelike crystals.
- On heat treatment, fibrillar crystals have a tendency to transform into lamellar crystals.[5,19] Phenomena of this type are also noted in other semicrystalline polymers.[34–38]
- Variation in the mechanical properties, long spacings measured from SAXS, lateral crystal size, crystallinity, melting behavior, shrinkage, and tan δ maximum peak temperature measured from DMA with HST follow a trend similar to that noted in Figure 1 for the biaxially oriented PET films.[6,7,12,20,35,39,40]
- A previous study led to the conclusion that the fibrillar crystals are embedded in an amorphous matrix. In this case, crystallites act as physical tie points in the network structure.[5]

DISCUSSION

Definition of Regimes and Optic Axis

To understand the variation in the film properties with HST, it may be useful to define temperature ranges according to the relaxation characteristics of

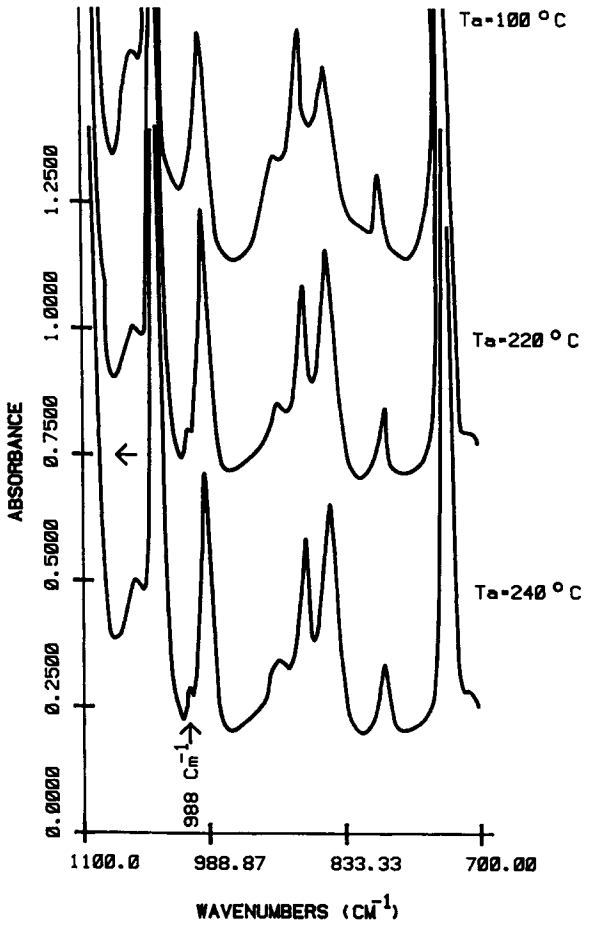

Figure 12 Infrared spectra of the films heat-set at different temperatures. T_a = annealing temperature.

PET molecules. The temperature range up to the stretching temperature, $T_g + C$, which is slightly higher than the glass transition temperature (T_g), can be considered as "Regime-I," while that from T_g up to the temperature where the maximum in crystallization rate (T_{max}) occurs can be considered as "Regime-II." The temperature from T_{max} to the melting temperature (T_m) can be defined as "Regime-III." The present study, thus, deals with the temperature range covering "Regime-II" and "Regime-III."

It is possible to arrive at generalizations regarding structural changes taking place along the OA of the film. Usually, the OA contains the maximum in the overall orientation of the molecules, as well as of the c-axis of the crystals. Note that the OA in the uniaxially oriented film will be along the MD, whereas in simultaneously biaxially stretched film with an equal draw ratio, it will be the same in all the directions within the plane of the films. In sequentially stretched films, the OA in the film plane is decided by the stretching parameters. In biaxially oriented films, the volume fraction of TD-oriented crystallites is determined from the stretching conditions.[1]

Crystalline Rearrangements with HST

In this section, it is our intention to carry out a general discussion of the nature of crystals and of the fusion process in Regime-II, as well as of the crystalline reorganization process via melting and recrystallization in Regime-III.

In previous papers, it has been shown that uni- and biaxially oriented PET films contain fibrillar or micellar crystals.[4,25,28] Electron microscopy of melt-deformed PET film also shows the presence of micellar crystals.[5] Such crystals have also been observed in biaxially oriented films.[1,3,4,22,28,29] The volume fraction of such crystals before heat treatment is in the range of 15–20%.

Our results indicate that during the heat treatment the (100) crystal plane preferentially orients into the film plane (Fig. 13). In addition, with increasing heat treatment, the percentage crystallinity as well as the lateral dimensions of crystallites also increase (Figs. 9 and 10). This suggests that the number of physical tie points increases with increasing heat treatment. Rearrangement in the crystals and their surrounding amorphous molecules occurs in such a fashion that SAXS gives distinct periodicities (Fig. 6 and Ref. 4). Fusion of the micellar crystals occurs below 180°C and the micellar character is maintained.[5] A typical fusion of fibrillar crystals of other semicrystalline polymers has already been noted well below the melting point.[19,33–36] In Regime-II, the increase in the lateral crystalline dimensions can impose a constraint on the oriented free molecules or the molecules interconnecting the crystallites.[2]

During heat treatment of the film (immediately after stretching in Regime-I) in Regime-III, the relatively more metastable crystals start melting (Fig. 11) and the existing crystals grow at the expense of metastable crystals. The general mechanism for the crystalline reorganization has been studied previously[10] and has been summarized in the previous section. Melting of the crystals starts destroying the initial network structure. The rate of the reorganization process via melting and recrystallization depends on the density of interconnecting tie molecules, their orientation, the temperature, and time. The IR study shows that the chain-folding concentration increases with HST. Thus, the nature of the

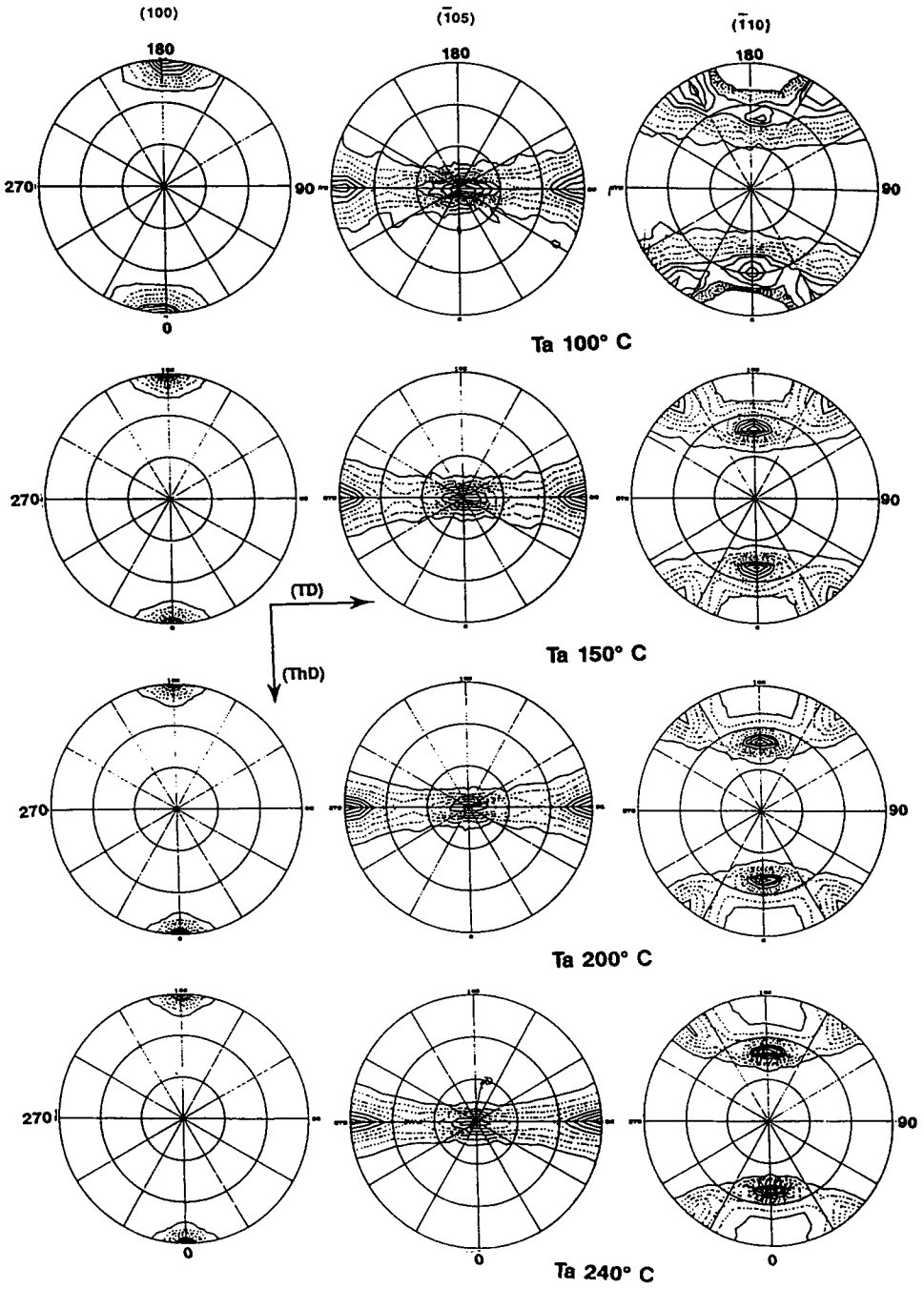

Figure 13 X-ray pole figures for the different crystal planes for the film heat-set at the different temperature. T_a = annealing temperature.

amorphous phase on the crystal surface will be a mixture of folded and nonfolded chains.

The rate of crystallization of PET from the relaxed state shows a maximum growth rate at 180°C.[41] This result is not applicable to the oriented polymeric systems. Studies of crystallization from the oriented state[42,43] indicate (a) an increase in the rate of crystallization by several orders of magnitude, and (b) that the temperature at which maximum crystallization occurs is shifted toward the melting point. In PET, the observed value for T_{max} is as high as 220°C. A recent crystallization study of fiber prepared from the melt confirms this conclusion.[42] We do not have data on kinetics of crystallization to

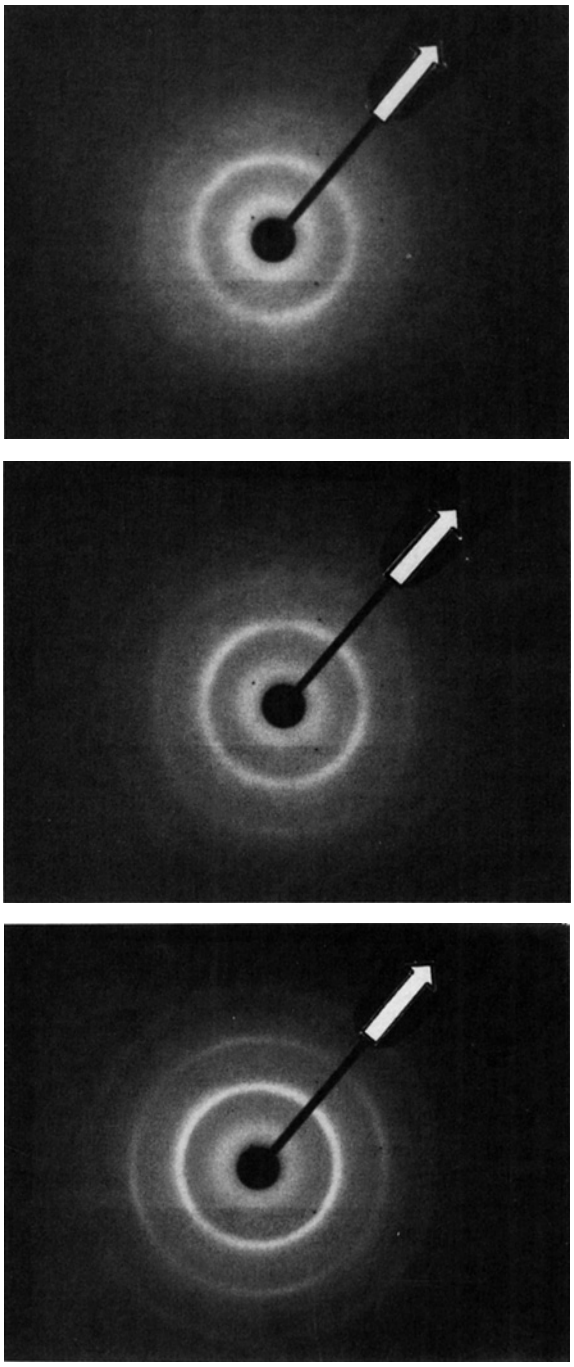

(a)

Figure 14 (a) X-ray diffraction pattern taken on the flat films. Note that diffraction becomes sharp with increasing HST. Arrow indicates the MD. (b) Diffractometer scans of the samples heat-set at different temperatures. Bars represent the counts. HW = half-width; T_a = annealing temperature.

confirm a similar trend in cold-drawn biaxially oriented films having isotropic in-plane molecular orientation. The occurrence of a transition in several properties, at about 180°C for biaxially stretched films with isotropic in-plane molecular orientation, coincides with the maximum in the rate of crystallization from the isotropic, relaxed molecular state. This suggests that at the very onset of the melting and recrystallization the molecular orientation starts slowly approaching that of the relaxed state and, therefore, crystallization follows a trend similar to that noted from the relaxed molten state. All the results lead to the conclusion that in Regime-II the higher rate of crystallization compared to the rate of molecular relaxation prevents molecular relaxation and, thus, constrains the amorphous phase.

Variation in the Amorphous Phase with HST

There is no direct method to elucidate the precise nature of the amorphous phase. For better understanding of the whole complex situation, it may be useful to summarize the major elements of the structural models: (a) the arrangement of interconnecting tie molecules between the crystallites; (b) the arrangement of free oriented molecules; and (c) the volume fractions of chain-folded and non-chain-folded crystals and their lateral sizes.

First, we consider the role of interconnecting tie molecules and their orientation in controlling the film properties.[16] It is always difficult to characterize the exact volume fraction of tie molecules and to correlate this with properties. A role of interconnecting tie molecules on the mechanical properties can be understood from the various structural situations shown in Figure 15. Two extreme simple arrangements of the interconnecting amorphous molecules with respect to the lamellar and the fibrillar crystals along OA (or along the draw direction) are shown in Figure 15. For simplicity, in these structural models, the distribution in the crystal thickness along the c-axis, as well as along the TD, is not shown. In fact, this parameter can also play an important role in the crystalline reorganization process. In Figure 15, there could be several intermediate stages; the precise nature of the structure in the films or fibers is determined from the molecular weight, polymer composition, the method of the stretching, and the processing parameters. Thus, the initial structure in the fibers or the films depends on the above-mentioned processing conditions. A relative idea of the structural arrangement can be deduced from the mechanical response. For example, a film having the A structure should manifest springlike or hard elastic fiber behavior,[44] whereas films having the D structure will behave like a short

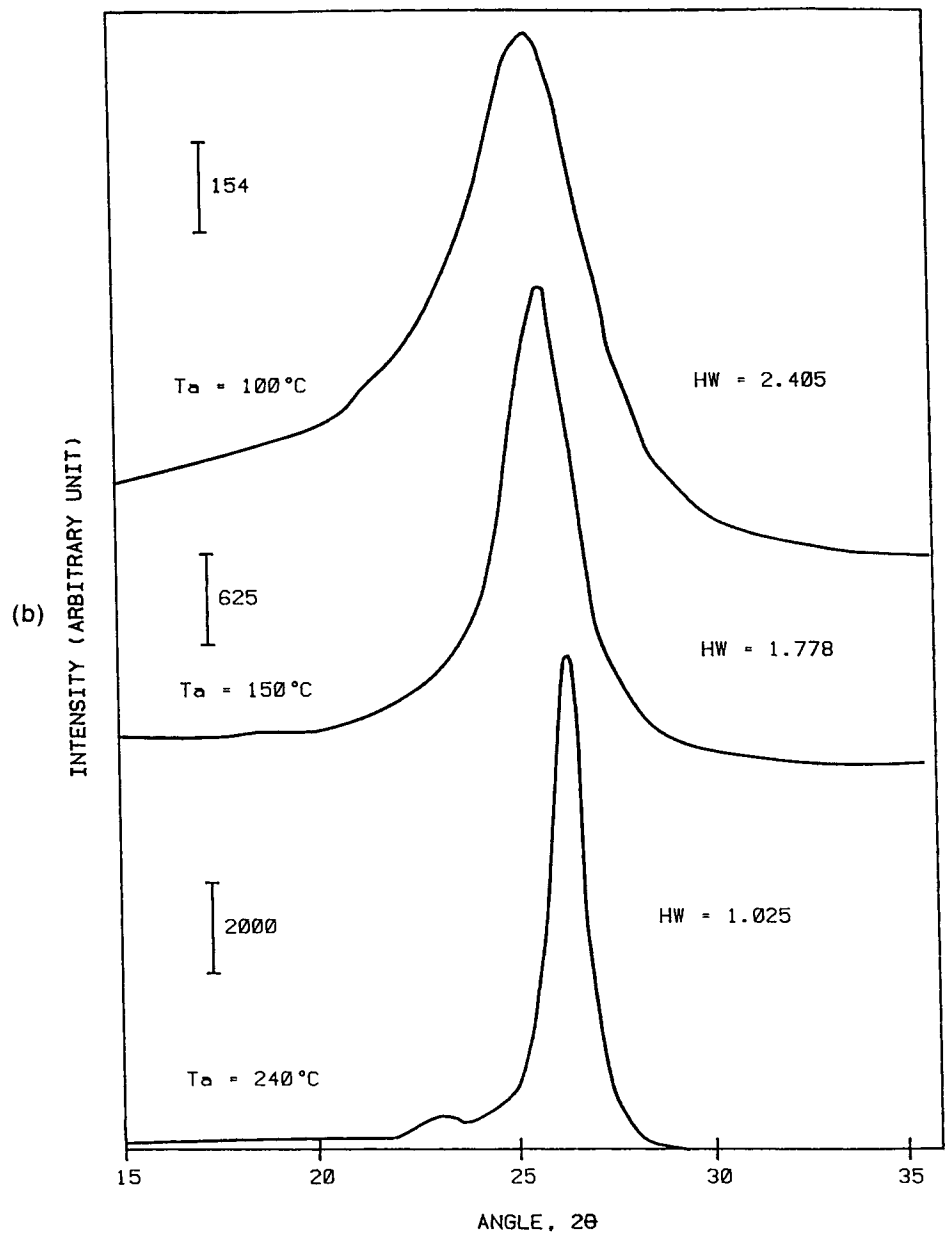

Figure 14 (*Continued from the previous page*)

fiber-reinforced composite.[31,32] Film having the B structure will be similar to that predicted in cold drawn ultrahigh modulus polyethylene.[45] In all models, the degree of interconnecting tie molecules and their orientation will determine the film properties.

The nature of the free molecules (molecules that have not taken part in the strain-induced crystallization process) can play an important role in the reorganization process. This particular structural element, as illustrated in Figure 16, has been included in fiber models.[8,46–48] It is difficult to characterize the nature and the arrangement of *free oriented molecules;* however, they can arise at a high draw ratio, particularly in a polymeric system having low crystallinity or in the non-heat-set films. These free amorphous molecules can have various degrees of orientation. Freedom of their motion in semicrystalline polymeric systems can be influenced by the percent crystallinity and the proximity of the surrounding crystals; the proximity of the crystal becomes more important when films are processed

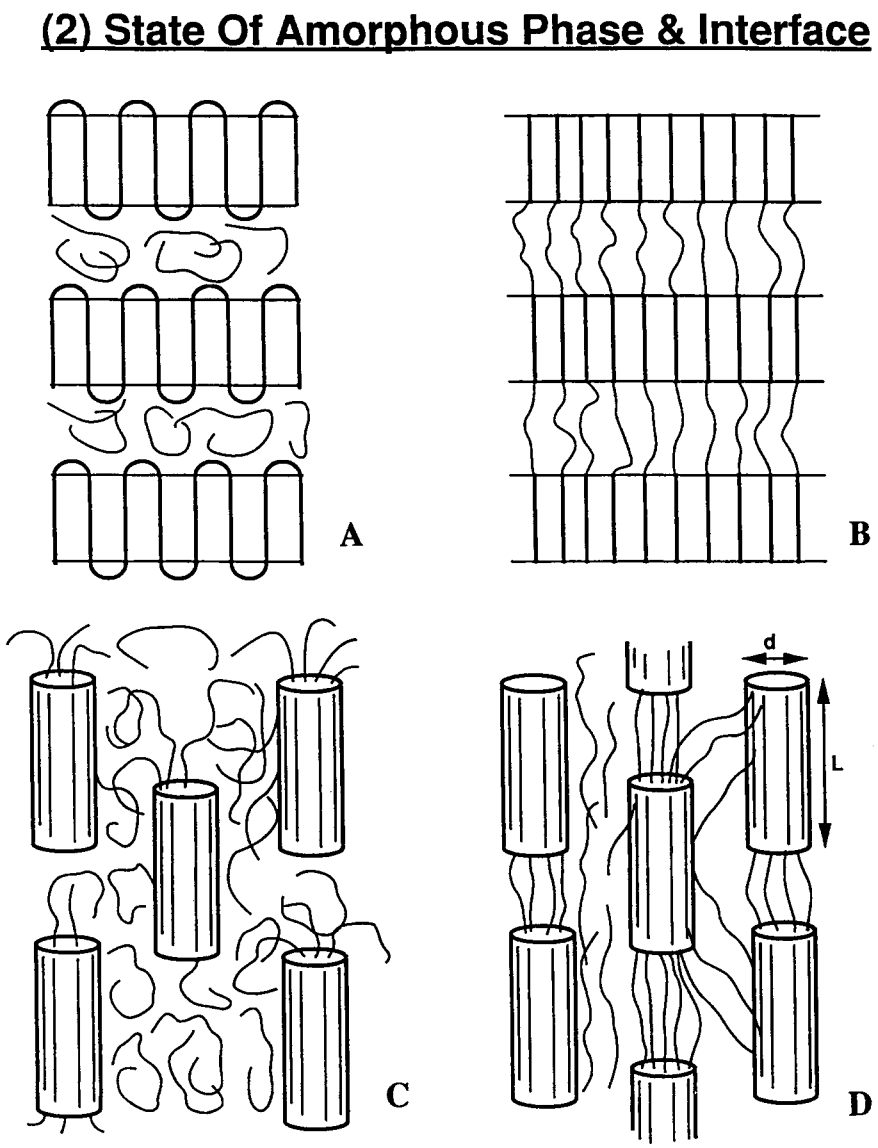

Figure 15 Schematic representation showing two extreme cases of the amorphous state in chain-folded lamellar crystals and needlelike extended chain crystals.

in Regime-II. In this condition, some free molecules can be envisaged as being locked among the crystallites. Previous studies[2,49] using DMA and oxygen permeability of uniaxially and biaxially oriented film with very low TD draw ratio gives an indication of the degree of constraint by crystallites on the oriented free molecules. This character is determined mainly from the processing conditions, i.e., degree of stretching and heat-setting. For example, such character will be less predominant in hard elastic fibers[44] but may be dominant in films prepared by cold drawing.[45] Annealing close to the melting point (where the melting and recrystallization predominates) of the films under no constraint or with fixed dimensions can reduce this character of the molecular constraint.

Structure of Uniaxially and Biaxially Oriented Films

In uniaxially oriented thin films, it is possible to deduce a fairly good picture regarding the nature of the crystals and their rearrangements during the heat treatment.[4,5,50] It is difficult, however, to depict a general model showing the exact arrangement of the amorphous phase. As discussed above, its nature is determined from the processing conditions for a sample of a particular molecular weight.

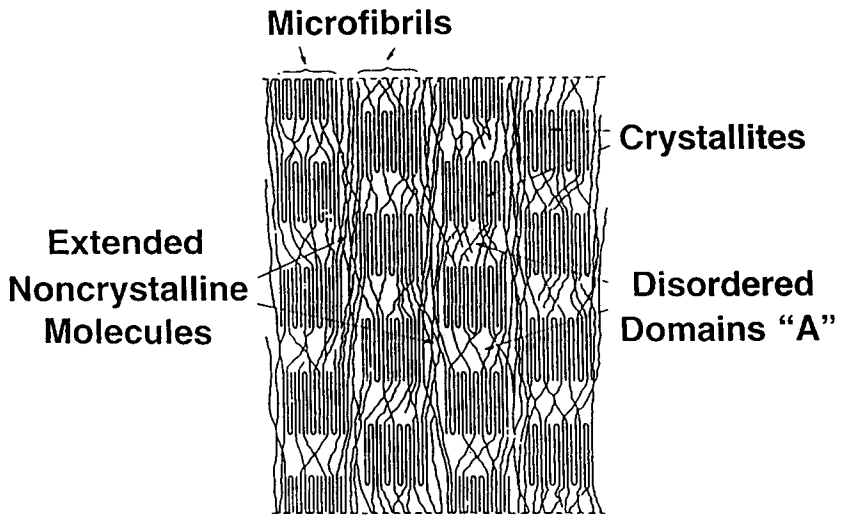

Figure 16 Schematic representation of PET fiber model showing crystallites, disordered domain, extended noncrystalline molecules, and microfibrils.[47]

In a previous article, we proposed a structural model for the uniaxially and sequential biaxially stretched films.[4] During the first uniaxial drawing at a temperature and with fixed strain rate, the c-axis of the crystallites coincides with the OA. With increasing TD draw, crystals start orienting toward TD and assume isotropic in-plane crystal orientation. At equal draw ratios, most of the crystals are oriented toward the TD. On heat treatment, the micellar crystallites having similar orientation start fusing to form lamellar-type crystals.[5,34,47]

We have also summarized the structural development during the simultaneous stretching process.[1,4] Our major results were consistent with those of other workers.[22,28,29] The basic nature of micellar- or fibrillar-type crystals is noted in uni- or biaxially oriented films.[5,25,28] During the heat treatment in Regime-II, as shown for the sequentially stretched films,[4] crystals with similar orientation try to fuse together, giving a lamellar appearance. Because of the high rate of crystallization in this regime, the initial molecular orientation is almost preserved. Looking to the variation in long spacing with HST in Regime-III, the melting and recrystallization process becomes predominant. Besides solid-state crystal thickening and the fusion processes, crystalline rearrangements take place via melting and recrystallization. The predominance of the melting and recrystallization process induces a relaxed amorphous phase, which is evident from Figures 5 and 8.

The structural situation in the different regimes is illustrated in Figure 17. The structure achieved after stretching close to T_g is shown in Regime-I. Depicted is an alignment of chains and crystallites along the OA in very local areas. (In simultaneously stretched films, the crystals are randomly oriented in the film plane.) The crystals are fibrillar in nature and are embedded in the amorphous matrix, forming an interconnecting network structure in which crystals act as physical tie points. Note that percent crystallinity at this stage is less than 20 and some oriented molecules do not take part in the strain-induced crystallization. The latter are termed "free molecules." Only in this regime, can physical aging occur.[51]

Heat treatment in Regime-II rapidly increases the physical tie points (percent crystallinity), crystal dimensions, and planarity. It should be remembered that the rate of crystallization (G) from the oriented state is several orders of magnitude higher than from the relaxed state. The rate of relaxation of molecules $(1/t)$ is lower in this regime and the higher rate of crystallization also prevents the relaxation of molecules. The growth of the new crystallites can impose a constraint on the molecules due to their close proximity and due to the increased number of physical tie points. Besides the crystal growth and solid-state crystal-thickening processes, fusion of micellar crystals will also occur in this regime. This situation leads to the development of a highly physically cross-linked network structure. In this type of structure, load can be easily transferred to the crystallites, as is apparent from strain hardening seen in Figure 2.

Molecular relaxation is induced when the initial structure in Regime-I is exposed directly to any temperature in Regime-III. It should be noted that metastable crystals will melt at these temperatures.

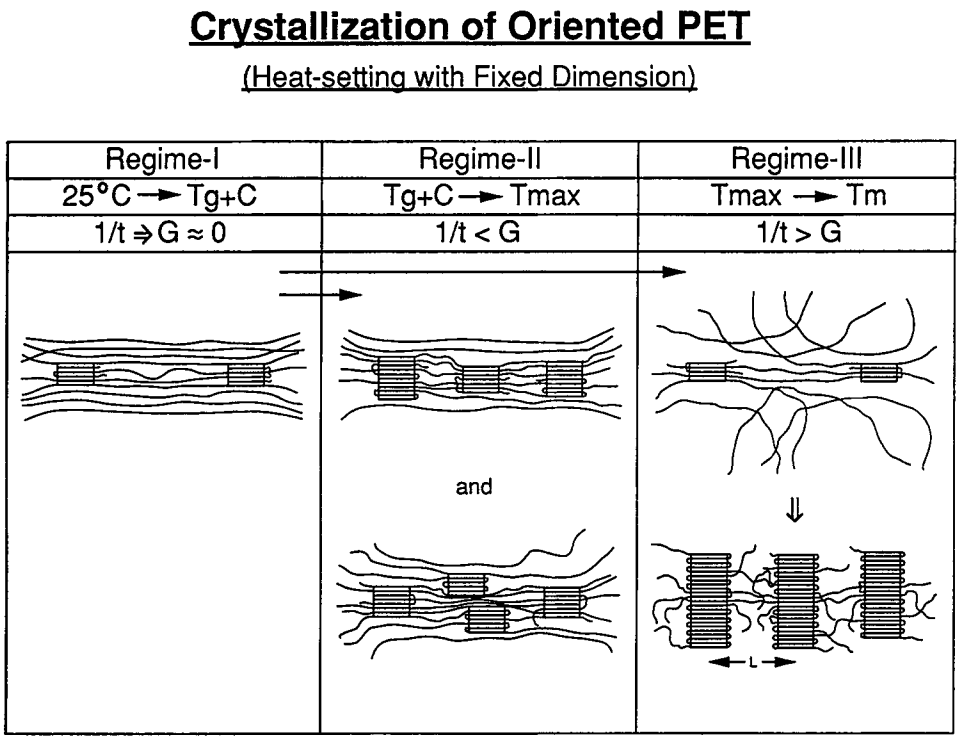

Figure 17 Schematic representation of structural situation in the various temperature regimes for the oriented film. L represents long spacings.

The development of a structure having more relaxed molecules is depicted in the Regime-III sketch. Compared to Regime-II, crystallization in this regime occurs from a state of relatively low orientation. Crystal growth from such a state will induce a lamellar morphology.[1,4] In this regime, long spacings become a strong function of heat-set temperature (Fig. 6). Further, the density of taut interconnecting tie molecules will decrease and a more relaxed amorphous phase will develop. With increasing heat-set temperature, the volume fraction of the amorphous phase also decreases, and this can make the material more brittle. The structural elements shown for the Regime-II are arranged along the OA and will show a structure similar to that shown in Figure 16 for the fiber and the uniaxially oriented films. In simultaneous biaxially stretched film, the crystallites as well as amorphous phase are randomly oriented in the film plane, as shown previously.[1-4]

Property Variation with HST

The observed transition in the several properties in the temperature range of 180–200°C in biaxially oriented film is similar to that noted in uniaxially oriented films and fibers. This implies that the major mechanism of structural reorganization is the same in both cases.

In "Regime-II," the increase in the values of tensile modulus, as well as stress at 5% strain, F-5 (Fig. 1), suggests an increase in the constraint in the amorphous phase. With increasing HST up to 180°C, the crystal dimensions and the crystallinity increases. As seen from the values of the tan δ maximum peak temperature, the constraint on the amorphous phase increases with HST. This increase in constraint is due to an increase in physical tie points (an increase in percent crystallinity), which form an effective network structure. Increased molecular constraint is also reflected in a decrease in the oxygen permeability and shrinkage.[2] This implies that during the crystallization process the molecular orientation does not change appreciably. This happens only under the condition that the rate of crystallization becomes equal or greater than the rate of molecular relaxation.

In "Regime-III," the values of tensile modulus and of F-5 decrease with HST (Fig. 3). The decrease in tan δ maximum peak temperature and increase in oxygen permeability and rate of hydrolysis suggest the development of a relaxed amorphous phase. This decrease in constraint occurs in spite of an increase in crystallinity. This is consistent with the mathe-

matical model of Buckley and Salem,[12] which shows that molecular constraints can decrease despite increasing crystallinity if accompanied by sufficient increases in chain folding and/or crystallite length. The increases in long spacings, measured from SAXS, and in chain folding, from FTIR, suggest considerable structural rearrangements of this type. In addition, there is a drastic decrease in film shrinkage, due to development of a relaxed amorphous phase. All the above results suggest that the melting and recrystallization process become predominant in this regime. At the same time, as HST increases to T_m, the rate of molecular relaxation increases while the rate of crystallization decreases.

From the above discussion, it is clear that to understand the changes in the properties of oriented fibers and films via reorganization during heat treatment it is necessary to consider the changes taking place in the molecular orientation as well as relative changes occurring in the two-phase structure due to competition among several processes, such as rates of crystallization, rates of molecular relaxation, solid-state crystal thickening, melting of crystals, as well as melting and recrystallization. In addition, for polyesters, the role of ester exchange reaction in the solid state requires attention; its role in the presence of trace amounts of catalytic residue may be appreciable when the films are annealed in "Regime-III."[19]

As shown above, predominance of a particular process in the different regimes can play an important role in the microstructural reorganization process and, thereby, in the properties. The rates of the reorganization processes in "Regime-III" can be changed by influencing any of the above-mentioned variables. For example, molecular relaxation in "Regime-III" can be reduced if the heat-set process is carried out under tension. The heat-setting of highly oriented systems under tension eliminates the concept of different regimes. Heat-setting under tension can increase rates of crystallization and reduce molecular relaxation. In addition, the decrease in entropy in the amorphous phase leads to superheating of crystals. Another way to achieve a constrained amorphous phase is to carry out restretching in Regime-III.[11] The development of a constrained amorphous phase will increase the values of tensile modulus and F-5. The structural changes during such a process are discussed by Fakirov and Evstatiev.[11]

The author is thankful to J. Barkley and R. Lee for their encouragement of this work. Experimental help of F. C. Frank and M. Keating is greatly appreciated.

REFERENCES

1. R. M. Gohil, *J. Appl. Polym. Sci.*, **48,** 1635 (1993).
2. R. M. Gohil, *J. Appl. Polym. Sci.*, **48,** 1649 (1993).
3. R. M. Gohil and D. R. Salem, *J. Appl. Polym. Sci.*, **47,** 1989 (1993).
4. H. Chang, J. M. Schultz, and R. M. Gohil, *J. Macromol. Sci.-Phys. B,* **32**(1), 99 (1993).
5. J. Petermann and U. Rieck, *J. Polym. Sci. Polym. Phys.*, **25,** 279 (1987).
6. Y. Mitsuishi and H. Tonami, *Sen-i Gakkaishi* (*J. Soc. Text. Cellulose Ind. Jpn.*), **20**(3), 140 (1964).
7. H. J. Oswald, E. A. Turi, P. J. Harget, and Y. P. Khanna, *J. Macromol. Sci.-Phys. B,* **13**(2), 231 (1977).
8. P. N. Peszkin, J. M. Schultz, and J. S. Lin, *J. Polym. Sci. Polym. Phys.*, **24,** 2591 (1986).
9. K. M. Gupte, H. Motz, and J. M. Schultz, *J. Polym. Sci. Polym. Phys.*, **21,** 1927 (1983).
10. E. W. Fischer and S. Fakirov, *J. Mater. Sci.*, **11,** 1041 (1976).
11. S. Fakirov and M. Evstatiev, *Polymer,* **31,** 431 (1990).
12. C. P. Buckley and D. R. Salem, *Polymer,* **28,** 69 (1987).
13. C. P. Buckley and D. R. Salem, *J. Appl. Polym. Sci.*, **41,** 1707 (1990).
14. V. B. Gupta and S. Kumar, *J. Appl. Polym. Sci.*, **26,** 1897 (1981); **26,** 1805 (1981).
15. K. Itoyama, *J. Polym. Sci. Part C Polym. Lett.*, **25,** 331 (1987).
16. R. Huisman and H. M. Heuvel, *J. Appl. Polym. Sci.*, **37,** 595 (1989).
17. V. B. Gupta, C. Ramesh, and A. K. Gupta, *J. Appl. Polym. Sci.*, **29,** 3115 (1984).
18. Y. Mitsuishi and M. Ikeda, *Kobunshi Kagaku,* **23**(253), 329 (1966).
19. J. M. Schultz and S. Fakirov, Eds., *Solid State Behavior of Linear Polyesters and Polyamides,* Prentice-Hall, Englewood, NJ, 1990.
20. S. Fakirov, *Structure and Properties of Polymers,* Sofia Press, Sofia, 1985.
21. Y. Maruhashi and T. Asada, *Polym. Eng. Sci.*, **32**(7), 481 (1992).
22. M. Cakmak, J. E. Spruiell, J. L. White, and J. S. Lin, *Polym. Eng. Sci.*, **27**(12), 893 (1987).
23. Y. Shimizu, E. Toba, S. Sekiguchi, and A. Konda, *Sen-i-Gakkaishi,* **44**(3), 111 (1988).
24. M. F. Vallat, D. J. Plazek, and B. Bhusan, *J. Polym. Sci. Polym. Phys.*, **24,** 2123 (1986); **26,** 555 (1988).
25. J. J. Klement and P. H. Geil, *J. Macromol. Sci.-Phys. B,* **5**(3), 505 (1971).
26. W. Perkin, *Polym. Bull.*, **19,** 397 (1988).
27. J. L. Koenig and S. W. Cornell, *J. Macromol. Sci.-Phys. B,* **1**(2), 279 (1967).
28. K. Matsumoto, H. Ieki, and R. Imamura, *Sen-I Gakkaishi,* **27**(12), 516 (1971).
29. K. Matsumoto, Y. Izumi, and R. Imamura, *Sen-I Gakkaishi,* **28**(6), 189 (1972).
30. J. Petermann, J. Miles, and H. Gleiter, *J. Macromol.*

Sci.-Phys. B, **12,** 393 (1976); *J. Polym. Sci. Phys. Ed.,* **14,** 555 (1976).
31. J. Petermann and R. M. Gohil, *J. Macromol. Sci.-Phys. B,* **16**(2), 177 (1979).
32. R. M. Gohil and J. Petermann, *J. Mater. Sci.,* **18,** 1719 (1983).
33. J. L. Koenig and M. J. Hannon, *J. Macromol. Sci.-Phys.,* **B1**(1), 119 (1967).
34. J. M. Schultz and J. Petermann, *Colloid Polym. Sci.,* **262,** 294 (1984).
35. J. M. Schultz, J. S. Lin, R. W. Hendricks, J. Petermann, and R. M. Gohil, *J. Polym. Sci. Polym. Phys. Ed.,* **19,** 609 (1981).
36. E. W. Fischer and H. Goddar, *J. Polym. Sci. Polym. Symp.,* **16C,** 4405 (1969).
37. A. Peterlin and A. Sakaoku, *Kolloid Z.,* **212,** 51 (1966).
38. R. M. Gohil, M. J. Miles, and J. Petermann, *J. Macromol. Sci.-Phys. B,* **21**(2), 189 (1982).
39. R. M. Gohil and J. Petermann, *Polymer,* **22,** 1612 (1981).
40. R. J. Samuels, *Structured Polymer Properties,* Wiley, New York, 1974.
41. F. van Antwerpen and D. W. van Krevelen, *J. Polym. Sci. Phys. Ed.,* **10,** 2423 (1972).
42. R. K. Gupta and K. F. Auyeung, *Polym. Eng. Sci.,* **29**(16), 1147 (1989).
43. R. Elenga, R. Sequela, and F. Rietsch, *Polymer,* **32**(11), 1975 (1991).
44. C. A. Garber and E. S. Clark, *J. Macromol. Sci.-Phys. B,* **4,** 499 (1970).
45. A. Cliferri and I. M. Ward, Eds., *Ultra-High Modulus Polymers,* Applied Science, London, 1977.
46. J. W. S. Hearle and R. M. Peters, *Fiber Structure,* Butterworths, London, 1965.
47. D. C. Prevorsek, Y. D. Kwon, and R. K. Sharma, *J. Mater. Sci.,* **12,** 2310 (1977).
48. A. Peterlin, *J. Mater. Sci.,* **6,** 490 (1971).
49. K. Matsumoto, H. Ieki, and I. Imamura, *J. Fiber Sci. (JPN),* **27**(2), 516 (1971).
50. G. Harburn, J. W. Lewis, and J. O. Warwicker, *Polymer,* **26,** 469(1985).
51. L. C. E. Struik, *Physical Aging in Amorphous Polymers and Other Materials,* Elsevier, New York, 1978.

Received June 7, 1993
Accepted October 23, 1993